Biomass Conversion and Biorefinery (2023) 13:6121–6131
https://doi.org/10.1007/s13399-021-01545-3

ORIGINAL ARTICLE

Kinetic and thermodynamic analysis of biodiesel and associated oil from *Jatropha curcas* L. during thermal degradation

Adeyinka S. Yusuff[1,2] · Dinesh P. Bangwal[1] · Afeez O. Gbadamosi[2] · Neeraj Atray[1]

Received: 1 March 2021 / Revised: 23 April 2021 / Accepted: 26 April 2021 / Published online: 4 May 2021

Abstract

Herein, *Jatropha curcas* seed oil, a non-edible plant oil, was employed as low-grade feedstock to make biodiesel via a two-step transesterification process. The *Jatropha curcas* oil (JCO) and its corresponding biodiesel (JCO-B) were characterized by FTIR and GC-FID analyses. Thermal stability experiments were conducted using thermogravimetry (TGA/DTG) technique at different heating rates of 5, 10 and 15 °C/min with a temperature range from 30 to 900 °C. Kinetic and thermodynamic characteristics of JCO and JCO-B were investigated. The TGA data were evaluated by the Flynn-Wall-Ozawa (FWO) and Vyazovkin kinetic models, and the reaction order was predicted by Avrami theory. The obtained JCO-B conformed to European standard EN 14103, while its FAME content was 97.51 wt.%. The TGA data fitted well to the FWO isoconversional model with average activation energies of 108.22 kJ mol^{-1} and 33.91 kJ mol^{-1} for JCO and JCO-B, respectively. Additionally, on average, reaction orders estimated by the Avrami model were 1.21 and 1.19 for JCO and JCO-B, respectively. Positive enthalpy change (ΔH) and Gibbs-free energy (ΔG) suggested an endothermic and nonspontaneous thermal degradation process, while the negative entropy change (ΔS) indicated a more ordered process and reaffirmed nonspontaneous reaction. The findings from this study indicated that the TGA/DTG technique could be used to predict the thermal and oxidation stability of biodiesel with respect to time.

Keywords Biodiesel · Kinetics · Thermal degradation · Thermodynamic · Transesterification

1 Introduction

The quest for alternative and renewable energy sources has recently gained attention in many parts of the world due to the increasing demand for fuel for several purposes, depletion and environmental issues associated with fossil fuel. Biodiesel, a biodegradable, eco-friendly and non-toxic fuel, can serve as a promising substitute to fossil diesel due to its low emission, higher cetane index and higher flash point [1]. Biodiesel is most commonly synthesized by transesterification of plant oil or animal fat with alcohol through various techniques such as common batch process, supercritical process, microwave-assisted and ultrasonic irradiation techniques [2, 3]. Among these techniques, transesterification by the batch process had been reported to be the most economical and simple method to produce biodiesel [2]. Biodiesel has been produced from three generations of feedstocks [4]. The first- and second-generation biodiesels were prepared from edible and non-edible plant oils [4], while third-generation biodiesel feedstocks are being sourced from algae [5]. Also, low-grade feedstocks such as waste cooking oil [2] and waste animal fat [6] have been investigated previously, and successful production of biodiesels with acceptable properties was reported. However, feedstocks from plant oils account for almost 75% of biodiesel synthesis [7], and various seed oils, including palm kernel, soybean, *Karanja*, castor, sunflower, *Kariya* and *Jatropha curcas*, are being utilized for its production.

Jatropha curcas L. is a species of flowering plant which belongs to a family of *Euphorbiaceae*, and it is commonly known as physic nut, Barbados nut or purging nut. *J. curcas* plant, as seen in Fig. 1a, is a semi-evergreen shrub or small tree which can achieve a height of 6 m or more and grow on marginal lands during the dry season, thus does not require much water [8, 9]. Its seeds (Fig. 1b) contain 27–40% (average: 34.4%) oil that can be converted to high-quality biodiesel

✉ Adeyinka S. Yusuff
yusuffas@abuad.edu.ng

[1] Biofuel Division, CSIR-Indian Institute of Petroleum, Dehradun, India

[2] Department of Chemical and Petroleum Engineering, College of Engineering, Afe Babalola University, Ado-Ekiti, Nigeria

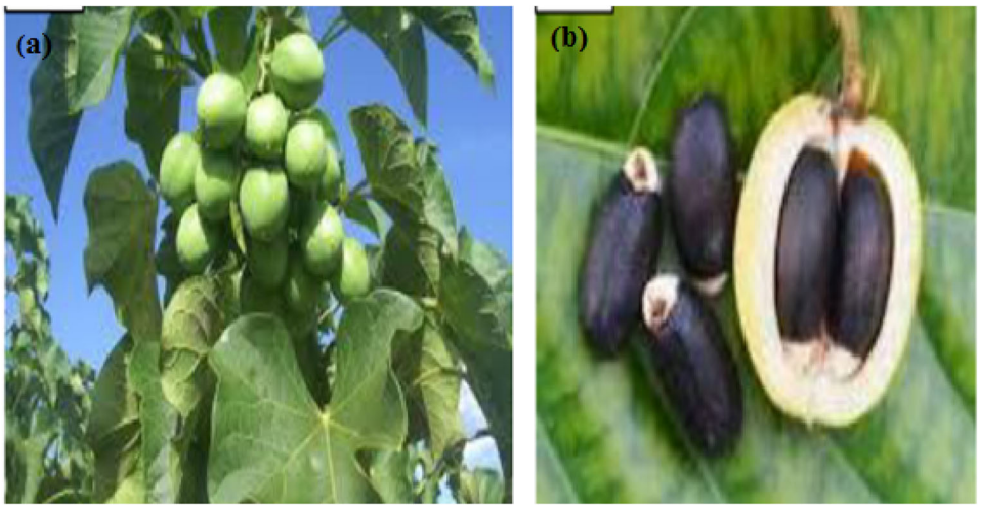

Fig. 1 *Jatropha curcas L.* **a** Plant and **b** seeds

fuel, usable in a standard diesel engine [10, 11]. *Jatropha curcas* showed excellent and sterling properties for biofuel production because of its desirable properties, higher oil content, longer life span and adaptation to dry and hot climates [12, 13]. *Jatropha curcas* oil (JCO) comprises various fatty acids with unsaturated components practically more than those of saturated compounds [14]. JCO is primarily made up of linoleic and oleic acids, which render the oil suitable for biodiesel production [15].

As a result of biodiesel importance globally and because of the various feedstocks that can be utilized to synthesize biodiesel, establishing specifications for industrial use of the raw materials is seen as an important step in achieving success and sustainability of biodiesel schemes. Biodiesel synthesized from any source must conform to established specifications such as ASTM, EN, Bureau of Indian Standards and other standard organizations [16, 17].

Oxidation stability, one of the biodiesel properties, has been receiving attention because biodiesel feedstocks are vulnerable to autoxidation. Therefore, biodiesels from such raw materials can quickly oxidize, which might result in high viscosity, acidity, density and so forth [18]. Moreover, degradation by oxidation results in products that impair fuel quality and engine performance [19]. The Rancimat method has been a standard technique for evaluating oxidation stability. However, several researchers have recently reported other methods that are faster and accurate [7, 20]. Most of the reported studies on evaluation of induction period (oxidation stability) considered differential scanning calorimetry (DSC) and pressure differential scanning calorimetry (PDSC) due to the oxidation process that is exothermic and reduced analysis period that is associated with DSC and PDSC compared to that of Rancimat methods [7, 21]. Therefore, these modern methods could be adopted to evaluate biodiesel oxidation stability as an aging time function [18].

Another characteristic of biodiesel that has gained tremendous attention is thermal stability, closely related to thermal degradation. Investigation of biodiesel's thermal stability could provide information regarding thermoxidative and kinetic parameters needed to predict the storage time of biodiesel samples and assess the engine performance [7, 18]. Several methods have been employed to determine biodiesel thermodynamic and kinetic parameters during thermal degradation, particularly the FWO, Friedman, Schneider Sestak-Berggren and Madhusudanan isoconversional methods, which depend on the degradation temperature and the extent of conversion [7, 22–25].

To investigate the reaction mechanism and thermodynamic behaviour of palm oil and its biodiesel during thermal degradation, Santos et al. [18] used Vyazovkin and FWO methods. Conceicao et al. [26] studied the thermal degradation of castor oil and biodiesel produced from the feedstock using methanol and ethanol as co-reactants. The authors reported the importance of investigating the reaction mechanisms involved during the material decomposition as the obtained kinetic parameters were used to predict the fuel storage time [26]. The kinetics and thermodynamic parameters of sunflower oil and its biodiesel during thermal degradation were evaluated using the Vyazovkin kinetic expression [21]. It is necessary to conduct thermal degradation studies on various feedstocks and their biodiesels to identify the appropriate isoconversional methods suitable for describing their kinetics and thermodynamic behaviours. So far, according to literature survey and to the best of our knowledge, kinetic and thermodynamic property studies of JCO and its corresponding biodiesel have not been considered. Thus, the main objectives of the current study were to investigate the thermal stabilities of JCO and its biodiesel (JCO-B) using Flynn-Wall-Ozawa and Vyazovkin kinetic models and to evaluate the kinetic and thermodynamic parameters of the oil and biodiesel from *Jatropha curcas* L.

2 Materials and methods

2.1 Materials

Jatropha curcas oil (JCO) used for this study was collected from the Biofuel Division, Indian Institute of Petroleum, India, while the reagents used, such as methanol (99.5%), potassium hydroxide (KOH, 84%), tetraoxosulphate (VI) acid (H_2SO_4, 98%), diethyl ether, ethanol (95%) and phenolphthalein, were purchased from Sigma-Aldrich Chemical Company, Mumbai, India.

2.2 Two-step transesterification process

A two-step transesterification, i.e., acid esterification followed by base transesterification, was adopted in this study to produce biodiesel due to high FFA content in the JCO. The acid esterification was conducted in a two-neck round bottom flask coupled with condenser and thermometer for temperature measurement using 60 mL of JCO, 30 mL of methanol and 0.1 mL of concentrated H_2SO_4 at 65 °C for 1 h. After the completion of the reaction, excess methanol, H_2SO_4 and water were removed from the product mixtures. The acid value of the JCO after esterification reaction was immediately determined using the titration method and found to have reduced to 1.04 from 11.2 mg KOH/g. Thereafter, the transesterification reaction was carried out after lowering the acid value of the oil (by acid esterification) using the same experimental setup. A total of 0.5 g of KOH was added to the required amount of methanol and shaken until it dissolved to form methoxide. The methoxide was thereafter added to the esterified JCO, and the reaction commenced immediately at 65 °C for 2 h. After the base transesterification process was completed, biodiesel was separated from the reaction products, washed with warm water and dried until the water was completely removed. The obtained biodiesel (JCO-B) was then kept in a covered container for analysis.

2.3 Analysis of JCO and JCO-B

The physicochemical characteristics of JCO and JCO-B (specific gravity, kinematic viscosity, acid value, FFA content, flash point, pour point and cloud point) were evaluated in line with the American Society for Testing and Materials (ASTM) procedures (see Table 1). The functional groups in JCO and JCO-B samples were determined with Fourier transform infrared (FTIR) spectrometer (Perkin Elmer-spectrum TWO, USA). FTIR spectra range was recorded from 4000 to 400 cm^{-1}. The methyl ester content in the JCO-B was analyzed using a gas chromatography (GC) coupled with a flame ionization detector (GC-FID, Agilent 7890A, USA). The GC column was a J & W DB-5HT capillary column of dimension 15 m × 0.32 mm × 0.10 mm with methyl heptadecanoate and helium gas as internal standard and carrier gas, respectively. A total of 10 μL of JCO-B was added to 100 μL of internal standard, and 1 μL of the mixture was injected into the analyzer. The oven temperature, which was initially set at 60 °C, increased to 180 °C at a heating rate of 15 °C/min, then rose to 230 °C at a heating rate of 7 °C/min and kept for 0 min. After that, the temperature was raised to 350 °C (set value of FID temperature) at 30 °C/min and held for 10 min.

Thermal stability studies on JCO and JCO-B were investigated using TGA/DTG thermogravimetric instrument (Shimadzu DTA 60, Japan) over the range of temperature of 30–900 °C under a nitrogen carrier gas with a flow rate of 60 mL/min and different heating rates of 5, 10 and 15 °C/min.

2.4 Kinetics and thermodynamic calculations

The data obtained from the thermogravimetric analysis at different heating rates (5, 10 and 15 °C/min) were evaluated using isoconversional kinetic models, namely FWO and Vyazovkin equations, to calculate some kinetic parameters such as activation energy (E_a), pre-exponential factor (A) and reaction order at the various extent of conversions ranging from 10 to 80%.

The influence of temperature on the degradation rate of the material involved could be expressed according to the following empirical equation:

$$g(\alpha) \equiv \int_0^{\alpha} \frac{1}{F(\alpha)} d\alpha = k(T)t \tag{1}$$

Introducing Arrhenius equation (Eq. 2a) in Eq. 1, we have

$$g(\alpha) = Aexp(-E_a/RT)t \tag{2a}$$

$$\int_0^{\alpha} \frac{d\alpha}{F(\alpha)} = g(\alpha) = A\beta^{-1}\int_0^{T} exp(-E_a/RT)dT \tag{2b}$$

Integrating Eq. (2b) and adopting Doyle's approximation [27], we have

$$g(\alpha) = \frac{A}{\beta} \times \frac{E_a}{R} \times 0.00484\exp\left(-1.052\frac{E_a}{RT}\right) \tag{3a}$$

$$\beta = \left(\frac{AE}{Rg(\alpha)}\right) \times 0.00484exp\left(-1.052\frac{E_a}{RT}\right) \tag{3b}$$

By Linearizing Eq. 3(b), it leads to Eq. 4,

$$ln\beta = ln\left(\frac{AE}{Rg(\alpha)}\right) - 5.331 - 1.052\frac{E_a}{RT} \tag{4}$$

Equation (4) is referred to as Flynn-Wall-Ozawa kinetic model. A plot of $ln\beta$ vs 1/T yields a straight line with slope$= -1.052\frac{E_a}{R}$.

where E_a is the activation energy (kJ mol^{-1}), A is the pre-exponential factor (min^{-1}), β is the heating rate (°C/min), R is

Table 1 Physicochemical and fuel properties of JCO and JCO-B

Property	Instrument/method used	ASTM test	Obtained value		ASTM D675 specification
			JCO[a]	JCO-B	
Specific gravity at 15 °C	D/08 Anton Parr densitometer	D4052	0.916	0.888	0.86–0.90
Kinematic viscosity at 40 °C (mm^2/s)	SVM 3001 kinematic viscometer	D445	37.8	5.6	1.9–6.0
Acid value (mg KOH/g)	Titration method	-	11.2	0.78	≤ 0.5
FFA content (wt.%)	Titration method	-	5.56	0.39	-
Flash point (°C)	GD-3536 Cleveland open-cup flash point tester	D93	256	183	≥ 130
Cloud point (°C)	K46100 C and P point chamber bath	D2500	+ 24	+ 12	-
Pour point (°C)	K46100 C and P point chamber bath	D97	+ 17	+ 7	-

[a] Yusuff [12]

the gas constant (8.314 J(K mol)$^{-1}$, T is the absolute temperature (K).

Vyazovkin model (Eq. 5) was also used to investigate the degradation of JCO and JCO-B.

$$ln\left(\frac{\beta}{T^2}\right) = \ln\left(\frac{AR}{E_a g(\alpha)}\right) - \frac{E_a}{RT} \tag{5}$$

Equation (5) proposes a non-linear isoconversional technique, unlike Eq. (4) which can only be used for linear heating rate conditions [22]. Furthermore, the reaction order, which describes thermal degradation in material, was evaluated using the Avrami model (Eq. 6).

$$\alpha = 1 - \exp\left(\frac{-K(T)}{\beta^n}\right) \tag{6}$$

By introducing Arrhenius equation (Eq. 2a) in Eq. (6), rearranging and linearizing each term, we have the following:

$$\ln(1-\alpha) = -Aexp\left(\frac{E}{RT}\right) \times \beta^{-n} \tag{7a}$$

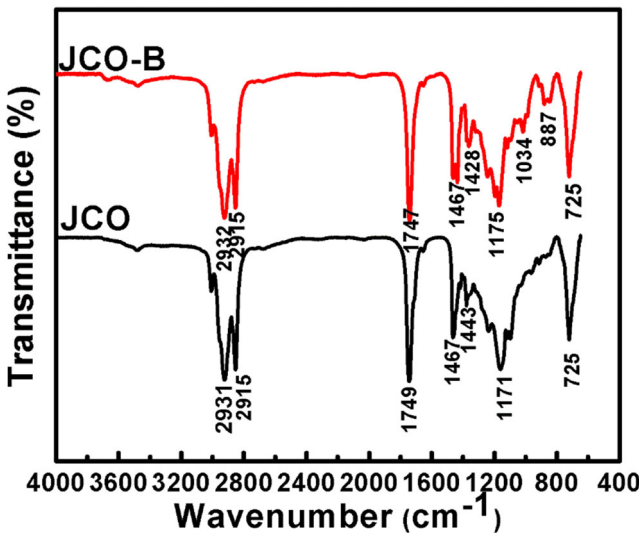

Fig. 2 FTIR spectra of JCO and JCO-B

$$-\ln(1-\alpha) = \beta^{-n} Aexp\left(\frac{E}{RT}\right) \tag{7b}$$

$$\ln(-ln(1-\alpha)) = \left(lnA - \frac{E}{RT}\right) - nln\beta \tag{8}$$

where n is the slope emanating from the plot of $\ln(-ln(1-\alpha))$ versus $ln\beta$ at the same temperature.

Moreover, since the thermal degradation of the two samples (JCO and JCO-B) was carried out at different heating rates, evaluation of thermodynamic parameters, such as enthalpy change (ΔH), Gibbs-free energy (ΔG) and entropy change (ΔS), was substantial to investigate the influence of heating rate on the degradation process. The ΔH, ΔG and ΔS can be determined by fitting experimental results at different conversions using the following equations:

$$\Delta H = E_a - RT \tag{9}$$

$$A = \beta \times \frac{E_a exp\left(\frac{E_a}{RT}\right)}{RT^2} \tag{10}$$

$$\Delta G = E_a + RT \times ln\left(\frac{K_B \times T}{h \times A}\right) \tag{11}$$

$$\Delta S = \frac{\Delta H - \Delta G}{T} \tag{12}$$

where K_B is the Boltzmann constant ($1.38 \times 10^{-23}\ J\ K^{-1}$) and h is the Plank constant ($6.626 \times 10^{-23}\ J\ s$)

3 Results and discussion

3.1 Physicochemical and fuel characteristics

Table 1 presents the results of the physicochemical analyses of the JCO and JCO-B. The results showed that two-step transesterification was required to convert the high FFA JCO to biodiesel as reaction would not occur if FFA content in the

Table 2 Fatty acid methyl ester composition of JCO-B

Methyl ester	Retention time (min)	Chemical structure	Composition (%)		Class
			JCO[a]	JCO-B	
Palmitic acid	12.873	C16:0	16.63	14.40	S
Palmitoleic acid	12.607	C16:1	1.05	0.86	US
Stearic acid	14.893	C18:0	6.62	12.11	S
Oleic acid	14.606	C18:1	53.27	37.54	US
Linoleic acid	14.699	C18:2	19.94	33.03	US
Others			2.49	2.06	
Total saturated (S) (%)			23.25	26.51	
Total unsaturated (US) (%)			74.26	71.43	

[a] Yusuff [12]

feedstock were above 3.0 wt.% [1]. However, the acid value of JCO-B (0.39 mg KOH/g), which conformed to the ASTM standard, was an indication that a significant amount of fatty acid in the oil had been converted. It is worth mentioning that no soap formation was noticed during second-stage transesterification due to the significant reduction of FFA content in the oil after acid esterification to 0.52 from 5.60 wt.%. A significant reduction in the kinematic viscosity of the produced biodiesel was noticed compared to that of the feedstock, which suggested a successful transesterification process. The kinematic viscosity value within 1.9–6.0 mm^2/s was desirable because viscous fuel resulted in engine performance problems such as coking of injector, wear and tear of injector and carbon deposition [28, 29].

Due to the lower molecular mass of biodiesel, the flash point of JCO-B was lower than that of JCO, indicating that the obtained biodiesel required less heat energy to vaporize. Furthermore, Table 1 reveals that the cold flow properties, in terms of the pour point and cloud point, reduced on transesterification of JCO and were conformed to their respective ASTM standard values.

3.2 FTIR analysis

To conduct a further investigation on JCO and JCO-B, the functional groups present in the samples were examined by FTIR analysis. Many similar absorption bands were noticed in the spectra of JCO and JCO-B (Fig. 2) due to chemical similarities that exist among triglycerides and esters [30]. The absorption bands at 2932, 2931 and 2815 cm^{-1} confirmed the presence of C–H asymmetric and symmetric stretching vibration [31], while typical absorption bands at around 1750 cm^{-1} and 1170 cm^{-1} were due to the stretching vibration of C=O ester and C–O ester, respectively [32]. However, a similar peak at 1467 cm^{-1} was noticed in the spectra of JCO and JCO-B, which could be attributed to the O–CH_3 deformation vibration. It is important to mention that new peaks were detected in the spectrum of JCO-B. The new peaks obtained at 1034 cm^{-1} and 887 cm^{-1} confirmed the presence of stretching vibrations of C–O (esters) and C–C, respectively. A similar band obtained at 725 cm^{-1} in the JCO and JCO-B spectra was due to overlapping of rocky vibration of $(CH_2)_n$ similar to observed peak in *Kariya* oil methyl ester [31].

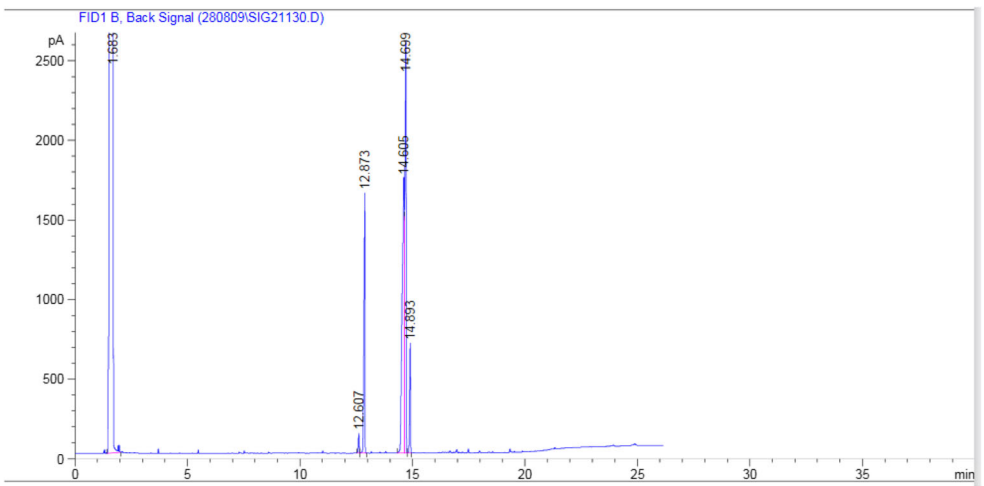

Fig. 3 Chromatogram of JCO-B

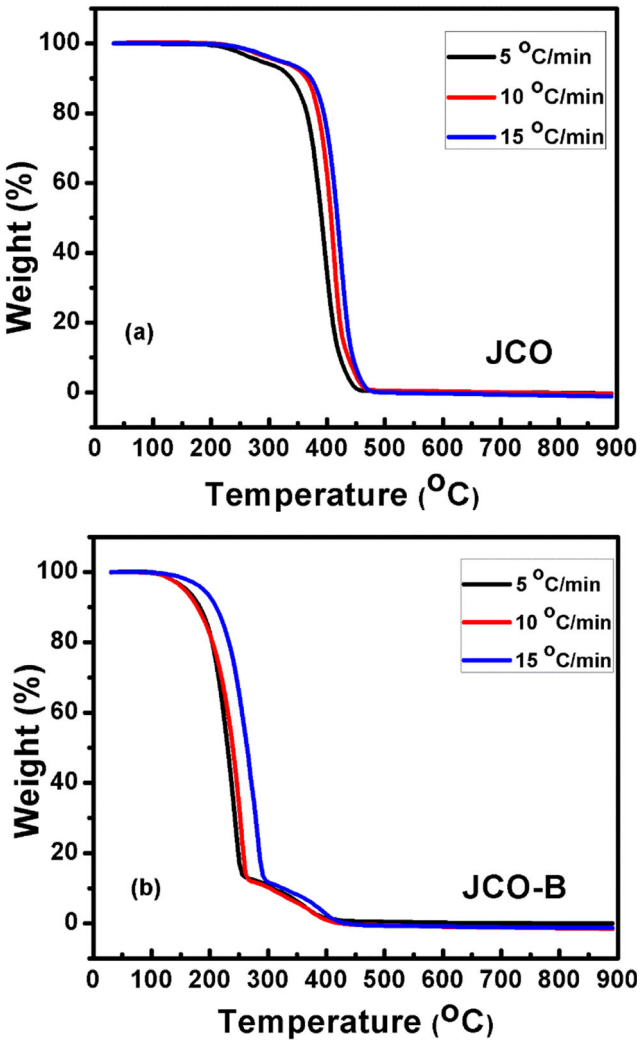

Fig. 4 TGA plots of **a** JCO and **b** JCO-B

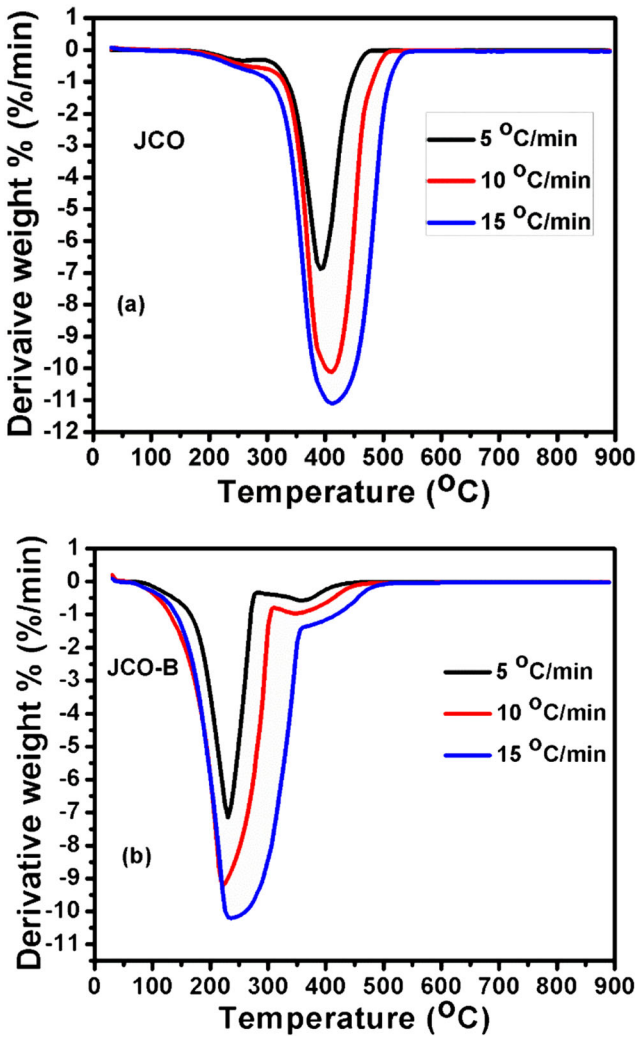

Fig. 5 DTG plot of **a** JCO and **b** JCO-B

3.3 FAME profile analysis

The chromatogram of methyl ester content in the JCO-B sample is shown in Fig. 3. Table 2, as expected base on the JCO composition, shows the dominance of methyl oleate (37.54%), methyl linoleate (33.03%) and methyl stearate (12.11%) in the JCO-B sample. Also, unsaturated methyl esters, which include methyl palmitoleate, oleate and linoleate, constituted 71.26% of the FAME content, thus indicating low biodiesel corrosivity and improved oxidation stability [33, 34]. The FAME content of 97.51 wt.%, which was higher than the European standard EN 14214 value (96.5 wt.%), corroborated the efficiency of two-step transesterification of high FFA JCO to produce methyl ester.

3.4 TGA analysis

In an attempt to gain insight into thermal degradation behaviours of JCO and JCO-B, both samples were subjected to thermal stability analysis using the TGA-DTG method. The typical TGA plots of JCO and JCO-B, which were not similar because of differences in molecular weights and intermolecular forces, are depicted in Fig. 4 a and b, respectively. As clearly observed in Fig. 4a, the TGA curves for JCO at different heating rates (5, 10 and 15 °C/min) exhibited a similar degradation trend with two mass loss stages observed. At the first stage of the decomposition, the mass loss rate was slow due to the volatilization of impurities and smaller molecules contained in the feedstock [7]. However, a significant weight loss was noticed in the temperature range of 331–462 °C, which could be attributed to the degradation of triglycerides. By taking everything into account, the percentage weight loss of 93.76% with a weight residue of 6.24% was recorded, as similar observations were reported for thermal degradation of palm oil [18], Brazilian sunflower oil [35] and castor oil [26].

The thermal decomposition of JCO-B at different heating rates (5, 10 and 15 °C/min) was also studied by the TGA technique, and experimental curves are displayed in Fig. 4b.

Table 3 Kinetics parameters and correlation coefficient (R^2) estimated using FWO and Vyazovkin models

Sample	∝ (%)	FWO model			Vyazovkin model		
		E_a (kJ mol^{-1})	A × 10^{13} (min^{-1})	R^2	E_a (kJ mol^{-1})	A × 10^{13} (min^{-1})	R^2
JCO	10	141.90	5.40	0.9995	140.97	4.85	0.9994
	20	119.48	4.17	0.9829	118.18	3.97	0.9805
	30	111.48	4.22	0.9889	109.39	4.01	0.9871
	40	130.42	3.08	0.9693	129.39	2.93	0.9655
	50	100.92	2.76	0.9995	104.21	2.81	0.8319
	60	93.99	1.29	0.9998	91.38	1.08	0.9998
	70	87.27	0.86	0.9986	84.48	0.82	0.9984
	80	79.77	0.65	0.9954	76.82	0.54	0.9946
JCO-B	10	69.09	0.48	0.7856	66.95	0.44	0.7565
	20	33.40	0.25	0.8267	30.32	0.23	0.7796
	30	32.76	0.18	0.8368	29.75	0.15	0.7918
	40	33.01	0.21	0.8465	30.72	0.19	0.8052
	50	33.05	0.22	0.8461	30.28	0.22	0.8061
	60	15.07	0.08	0.8278	29.81	0.20	0.7849
	70	29.86	0.03	0.7492	27.22	0.09	0.6913
	80	25.03	0.01	0.6302	22.36	0.04	0.5512

From the figure, it could be observed that TGA curves exhibited two stages of mass loss with a similar trend, as also observed in TGA plots of JCO. However, the degradation behaviour of JCO-B was different from that of the JCO sample, probably due to differences in molecular weight, as also reported in the case of palm oil and its corresponding biodiesel [18]. The major weight loss of 85.38%, being attributed to the isomerization and polymerization of methyl ester content in the JCO-B, took place in the range of 130 to 260 °C compared to the JCO degradation that occurred at a higher temperature. This observation indicated that JCO-B was less thermally stable than JCO, attributing to the fact that the biodiesel from *Jatropha* oil possessed a lower molecular weight, lower viscosity and weaker intermolecular forces [36]. In the second stage of the degradation, a weight loss of 11.96% was noticed over the temperature range of 260 to 390 °C, which was attributed to the loss of higher molecular weight methyl esters and other compounds in the sample. The overall percentage weight loss and weight residue were 96.34% and 3.66%, respectively. It was worthy of note that the thermal degradation of JCO-B was completed at around 400 °C while that of JCO ended at 461 °C. The difference could be attributed to the fact that the flash point of biodiesel was lower than that of its feedstock [18].

3.5 DTG analysis

Figure 5 shows the DTG curves of JCO and JCO-B with bimodal structure commensurate with TGA plots. As the temperature increased, the values of DTG were correspondingly heightened, suggesting that the thermal decomposition rate proceeded faster until the maximum mass loss rate (DTG_m) was attained. Thereafter, the DTG value almost became zero as thermal decomposition was completed. However, as evident in Fig. 5b, the thermal degradation rate was suddenly disturbed at around 300 °C before it picked up again until the curve become flattened. The reason for this observation was that JCO-B contained methyl esters with different molecular weights. It is important to mention that the thermal decomposition of both samples was delayed as the heating rate increased due to the limitation of heat transfer [7]. The DTG_m became more significant as the heating rate was increasing. For example, the DTG_m of JCO at 5 °C/min, 10 °C/min and 15 °C/min was 6.88%/K, 9.83%/K and 10.83%/K, respectively. Even thermal degradation of JCO-B at different heating rates followed the same trend.

3.6 Thermal degradation kinetics

Kinetics of JCO and JCO-B degradation was carried out by applying FWO and Vyazovkin models to test thermal degradation data. Thus, the kinetics of the thermal decomposition process was elucidated. To evaluate some kinetic parameters (activation energy (E_a), pre-exponential factor (A), reaction order (n) and corresponding correlation coefficient (R^2)), different values of conversion from 10 to 80% were chosen at an interval of 10% at various heating rates of 5, 10 and 15 °C/min. The plot of $In\beta$ against 1000/T (Fig. 6 a and b) revealed that the degradation of JCO and JCO-B obeyed the

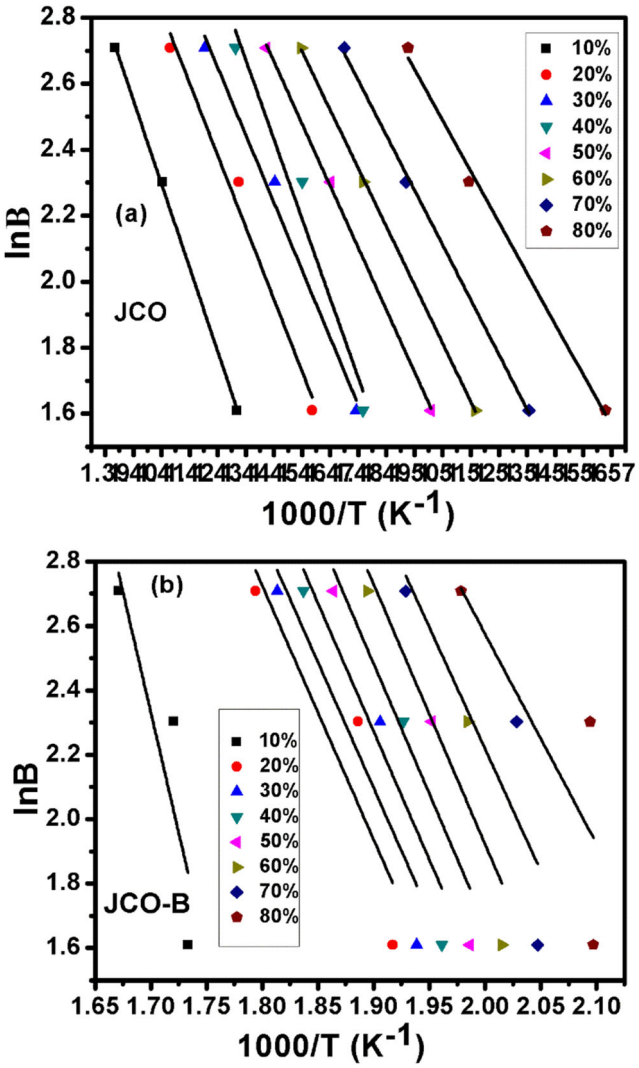

Fig. 6 Flynn-Wall-Ozawa kinetics for thermal degradation of **a** JCO and **b** JCO-B

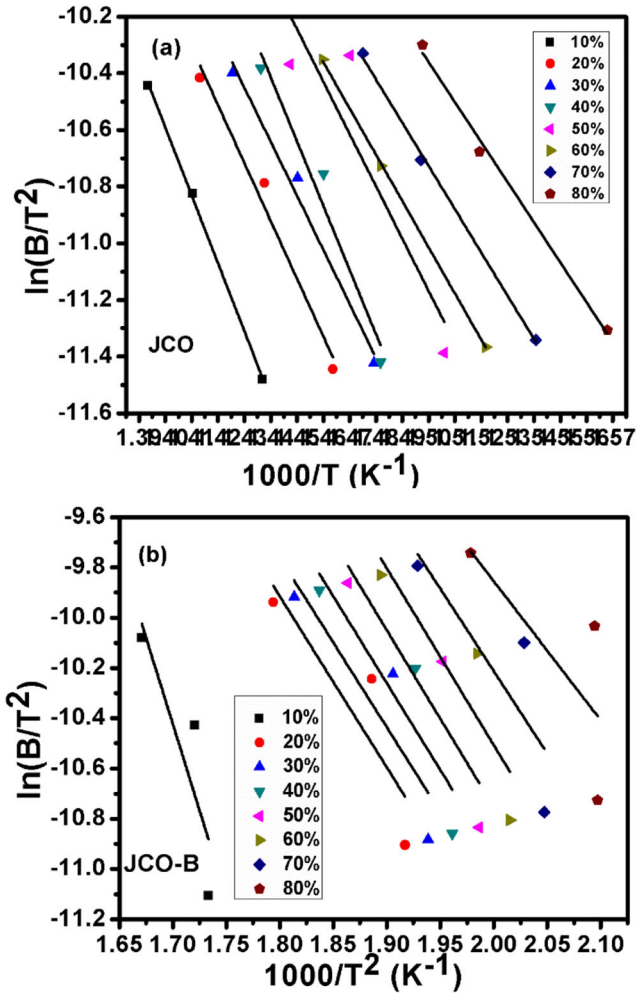

Fig. 7 Vyazovkin kinetics for thermal degradation of **a** JCO and **b** JCO-B

FWO model. The kinetic parameters E_a and A were estimated from the slope and intercept of the graphs and are presented in Table 3. The R^2 values (0.9693–0.9995 and 0.6302–0.8465) for JCO and JCO-B, respectively, suggested that the FWO isoconversional model provided a good fit to the degradation data. A similar result was documented for the thermal degradation of palm oil and its biodiesel [18]. Furthermore, the values of E_a and A were determined from the slope and intercept of the Vyazovkin model plots (Fig. 7 a and b) and are presented in Table 3. This observation gave an indication that the Vyazovkin model was a non-linear isoconversional kinetic expression, as also confirmed by Vyazovkin [37]. The best thermal degradation kinetic model was chosen based on the linear square regression correlation coefficient (R^2). As evident in Table 3, it was noticed that the thermal degradation data for JCO and JCO-B fitted reasonably well to the FWO isoconversional model, which confirmed the linear heating rate conditions [22].

Activation energy, being an energy barrier, needs to be overcome for a reaction to proceed to completion and a higher value suggests a complex reaction process [36]. Thermal decomposition rate is a function of activation energy as it evaluates the progress and sensitivity of reaction. As evident in Table 3, E_a values of JCO-B estimated by FWO and Vyazovkin techniques were found to be in the range of 15–70 kJ mol^{-1} and 22–67 kJ mol^{-1}, respectively. By comparing

Table 4 Reaction order for thermal degradation of JCO and JCO-B

JCO			JCO-B		
Temperature (K)	n	R^2	Temperature (K)	n	R^2
424	1.20	0.9275	393	1.13	0.9112
474	1.33	0.9868	423	1.47	0.9999
579	1.12	0.9378	474	1.34	0.9874
624	1.27	0.9363	513	1.03	0.9240
674	1.13	0.9933	573	1.01	0.9081
Average value	1.21			1.19	

Table 5 Estimated thermodynamic parameters of JCO and JCO-B during thermal degradation

Sample	∝ (%)	FWO model			Vyazovkin model		
		ΔH (kJ mol^{-1})	ΔG (kJ mol^{-1})	ΔS (J mol^{-1} K^{-1})	ΔH (kJ mol^{-1})	ΔG (kJ mol^{-1})	ΔS (J mol^{-1} K^{-1})
JCO	10	136.02	76.34	84.35	135.09	94.83	56.89
	20	114.20	75.71	55.33	112.39	93.94	26.53
	30	105.75	75.27	44.24	103.66	93.35	14.96
	40	124.72	73.88	74.19	123.69	91.80	46.53
	50	95.28	72.95	32.91	98.57	91.92	9.81
	60	88.40	73.99	21.44	85.79	91.68	− 8.76
	70	81.74	73.40	12.54	78.95	90.93	− 18.01
	80	74.32	72.49	2.81	71.38	89.77	− 28.09
JCO-B	10	64.22	30.28	57.95	62.95	79.34	− 29.47
	20	28.94	29.81	− 1.63	25.86	75.05	− 91.70
	30	28.35	29.43	− 2.05	25.34	43.71	− 34.61
	40	28.65	28.91	− 0.49	25.76	73.11	− 90.28
	50	28.75	28.34	0.79	25.99	42.21	− 31.36
	60	10.83	31.02	− 39.64	23.58	70.67	− 88.53
	70	25.70	27.38	− 3.35	23.07	69.15	− 92.16
	80	20.98	27.03	− 12.43	18.31	68.13	− 102.38

these E_a values of JCO-B with those of JCO sample, it was noticed that the thermal degradation of JCO was complex due to higher activation energies (79–142 kJ mol^{-1}) for the FWO model and 76–141 kJ mol^{-1} for the Vyazovkin model. The decomposition of JCO took place at higher activation energy due to its higher molecular mass, higher viscosity and stronger intermolecular forces. It is worthy of note that no much difference was observed between the two isoconversional models, thus indicating that many kinetic expressions could be employed to estimate E_a in as much as they are adequately chosen.

The reaction orders of thermal degradation for JCO and JCO-B, which were determined through the Avrami kinetic model, are listed in Table 4. The n values were found to be in the range 1.13–1.33 for JCO and 1.01–1.47 for JCO-B. Moreover, the variation between the estimated average n values of JCO and JCO-B was insignificant for the Avrami model, indicating that the thermal degradation was not complex and suggesting that no side reactions were involved [7]. However, the variation trend of n for both samples was not consistent with temperature accretion. For example, with temperature increase, n for JCO increased from 1.20 to 1.33 and then decreased to 1.12, at the temperature of 579 K. The same trend was noticed in the case of JCO-B. A similar result had been documented by Li et al. [7] during thermal degradation of rapeseed biodiesel and its blends with diesel, where the kinetic characteristics evaluation at different heating rates revealed inconsistency in the values of reaction orders obtained.

However, the R^2 values (0.9275–0.9933 for JCO and 0.9112–0.9999 for JCO-B) were generally high for all n values for the Avrami kinetic expression. As such, the reaction orders of thermal degradation of JCO and JCO-B could be best predicted by the Avrami kinetic model.

3.7 Thermal degradation thermodynamics

Thermodynamic parameters of JCO and JCO-B degradation, including enthalpy change (ΔH), Gibbs free energy change (ΔG) and entropy change (ΔS), were estimated to investigate thermodynamic characteristics of oil and biodiesel from *Jatropha curcas L*. Table 5 presents the estimated values of thermodynamic parameters for JCO and JCO-B samples. The positive values of ΔH, as seen in Table 5, suggested that the thermal degradation process was endothermic. The ΔH values for JCO are greater than those values for JCO-B. This indicates high reactivity of biodiesel as compared to oil with low reactivity [38, 39]. This observation further confirmed that JCO was thermally stable than the JCO-B.

Also, the Gibbs free energy was calculated, and thermal decomposition for either JCO or JCO-B sample was non-feasible and nonspontaneous due to ΔG values that were all positive. Additionally, the decline in ΔG values with an increase in extent of degradation indicated a rapid thermal degradation at a higher temperature. It was worthy of note that values of ΔG for the two samples estimated by the two isoconversional techniques revealed a decreasing trend, though not consistent. For instance, ΔG of JCO calculated

by the FWO method was decreased from 76.34 to 72.95 kJ mol^{-1} and then increased to 73.99 kJ mol^{-1}. Also, ΔG estimated using the Vyazovkin method showed a similar variation trend. Besides, the same trend was observed in ΔG of JCO-B for both FWO and Vyazovkin models. On the basis of average, ΔG of JCO estimated by the FWO and Vyazovkin models were 74.25 and 92.28 kJ mol^{-1}, respectively. As for JCO-B, the mean ΔG estimated by the FWO and Vyazovkin models were 29.03 and 65.17 kJ mol^{-1}, respectively. By comparing these values, it was noticed that JCO had higher ΔG values compared to JCO-B, which suggested lower favourability of reaction.

Entropy change (ΔS), the degree of disorderliness of a system, was also estimated by the FWO and Vyazovkin methods. As seen in Table 5, the ΔS values for JCO calculated by FWO method were all positive, whereas some negative ΔS values were obtained for JCO calculated by the Vyazovkin method. On the other hand, except for ΔS value calculated by FWO at the conversion of 10%, values of ΔS for JCO-B calculated by FWO and Vyazovkin models at various conversions were all negative. However, the positive value of ΔS suggested an increase in irregularity and randomness of a reactant during thermal degradation, while a negative ΔS indicated that the disorder of the degradation process had decreased. On average, ΔS values for JCO calculated by FWO and Vyazovkin methods were 40.98 and 12.48 J mol^{-1} K^{-1}, respectively, whereas average values of ΔS for JCO-B calculated by the FWO and Vyazovkin were − 0.11 and − 70.01 J mol^{-1} K^{-1}, respectively. Based on these calculated values, it could be presumed that the thermal degradation of JCO was spontaneous while that of JCO-B was a non-spontaneous process. The negative ΔS values obtained for thermal degradation of JCO-B agree with the works reported by Niu et al. [25], Li et al. [7] and Rodrigues et al. [39], who mentioned that ΔS values during thermal decomposition of biodiesel either in the presence or absence of oxygen were negative. Based on results obtained, it could be concluded that less energy was needed for JCO-B to reduce the degree of disorder due to its average ΔS value that was found to be negative in comparison with average ΔS value of JCO that was positive.

4 Conclusion

Kinetic and thermal degradation characterization of JCO and its corresponding biodiesel were successfully evaluated. JCO was thermally stable than JCO-B due to its higher molecular weight and stronger hydrogen bond. Thermal analysis data fitted reasonably well to FWO kinetic method with an average E_a of 108.22 and 33.91 kJ mol^{-1} for JCO and JCO-B, respectively. The activation energy for the thermal decomposition of JCO was higher than that of JCO-B, indicating the complexity of JCO degradation, probably due to side reactions involved. Positive ΔH and ΔG confirmed the endothermic and nonspontaneous thermal degradation process while the negative ΔS indicated a more ordered process and reaffirmed nonspontaneous reaction. The obtained results showed that thermal stability analysis could provide the information needed to understand the thermoxidative and kinetic behaviours of biodiesel and its feedstock, which are necessary to assess the engine performance.

Acknowledgements The first author (Dr. Adeyinka Sikiru Yusuff) gratefully acknowledged the CSIR-TWAS fellowship award (FR number: 3240306317) for postdoctoral research at CSIR-Indian Institute of Petroleum, India.

References

1. Tan YH, Abdullah MO, Hipolito CN, Taufiq-Yap YH (2015) Waste ostrich and chicken-eggshells as heterogeneous base catalyst for biodiesel production from used cooking oil: catalyst characterization and biodiesel yield performance. Appl Energy 2:1–13
2. Avinash A, Murugesan A (2017) Chemometric analysis of cow dung ash as an adsorbent for purifying biodiesel from waste cooking oil. Sci Rep 7:9526
3. Murugesan A, Subramaniam D, Avinash A, Nedunchezhian N (2015) Quantitative and qualitative analysis of biodiesel- an in-depth study. Int J Ambient Energy 36(1):19–30
4. Sekar M, Mathimani T, Alagumalai A, Chi NTL, Duc PA, Bhatia SK, Brindhadevi K, Pugazhendi A (2021) A review on the pyrolysis of algal biomass for biochar and bio-oil-Bottlenecks and scope. Fuel 281(1):119190
5. Jacob A, Ashok B, Alagumalai A, Chyuan OH, Le PTK (2021) Critical review on third generation micro algae biodiesel production and its feasibility as future bioenergy for IC engine applications. Energy Convers Manag 228:113655
6. Lawan I, Garba ZN, Zhou W, Zhang M, Yuan Z (2020) Synergies between the microwave reactor and CaO/zeolite catalyst in waste lard biodiesel production. Renew Energy 145:2550–2560
7. Li H, Liu F, Ma X, Cui P, Gao, Yu M, Guo M (2019) Effects of biodiesel blend on the kinetic and thermodynamic parameters of fossil diesel during thermal degradation. Energy Convers Manag 198:111930
8. Mouahid A, Bouanga H, Crampon C, Badens E (2018) Supercritical CO_2 extraction of oil from Jatropha curcas: an experimental and modeling study. J Supercrit Fluids 141:2–11
9. Martinez A, Mijangos GE, Romero-Ibarra IC, Hernandez-Altamirano R, Mena-Cervantes VY (2019) In-situ transesterification of Jatropha curcas L. seeds using homogeneous and heterogeneous basic catalysts. Fuel 235:277–287
10. Achten WMJ, Mathijs E, Verchot L, Singh VP, Aerts R, Muys B (2007) Jatropha biodiesel fueling sustainability. Biofuels Bioprod Biorefin 1(4):283–291
11. Achten WMJ, Verchot L, Franken YJ, Mathijs E, Singh VP, Aerts R, Muys B (2008) Jatropha biodiesel production and use. Biomass Bioenergy 32(12):1063–1084
12. Yusuff AS (2021) Parametric optimization of solvent extraction of Jatropha curcas seed oil using design of experiment and its quality characterization. South Afr J Chem Eng 35:60–68
13. Hamzah NHC, Khairuddin N, Siddique BM, Hasan MA (2020) Potential of Jatropha curcas L. as biodiesel feedstock in Malaysia: a concise review. Processes 8:786–797

14. Kumar R, Das N (2018) Seed oil of Jatropha curcas L. germplasm: analysis of oil quality and fatty acid composition. Ind Crop Prod 124:663–668
15. Nzikou JM, Matos L, Mbemba F, Ndangni CB, Panboutobi NPG, Kimbonguila A, Silou TH, Linder M, Desobry S (2009) Characterization and composition of *Jatropha curcas* oils, variety Congo-Brazzavile. Res J Appl Sci Eng Technol 1(3):154–159
16. Yusuff AS, Adeniyi OD, Olutoye MA, Akpan UG (2017) A review on application of heterogeneous catalysts in the production of biodiesel from vegetable oils. J Appl Sci Process Eng, 2017 4(2):142–157
17. Ho WWS, Ng HK, Gan S, Tan SH (2014) Evaluation of palm oil mill fly ash supported calcium oxide as a heterogeneous base catalyst in biodiesel synthesis from crude palm oil. Energy Convers Manag 8:1167–1178
18. Santos AGD, Souza L, Caldeeira VPS, Farias MF, Fernandes VP Jr (2014) Kinetic study and thermoxidative degradation of palm oil and biodiesel. Thermochim Acta 592:18–22
19. Pullen J, Saeed K (2012) An overview of biodiesel oxidation stability. Renew Sust Energ Rev 16(8):5924–5950
20. Silver WC, Castro MPP, Perez VH, Machado FA, Mota L, Sthel MS (2016) Thermal degradation of ethanolic biodiesel: physicochemical and thermal properties evaluation. Energy 114:1090–1090
21. Santos AGD, Caldeira VPS, Farias MF, Araujo AS, Souza LD, Barros AK (2011) Characterization and kinetic study of sunflower oil and biodiesel. J Therm Anal Calorim 106:747–751
22. Vyazovkin S, Wight CA (1998) Isothermal and non-isothermal kinetics of thermally stimulated reaction of solids. Int Rev Phys Chem 17(3):407–433
23. Vyazovkin S, Sbirrazzuoli N (2006) Isoconversional kinetic analysis of thermally stimulated processes in polymers. Molecular Rapid Commun 27:1515–1532
24. Kaur R, Gera P, Jha MK, Bhaskar T (2018) Pyrolysis kinetics and thermodynamic parameters of castor (Ricinus communis) residue using thermogravimetric analysis. Bioresour Technol 250:422–428
25. Niu S, Yu H, Zhao S, Zhang X, Li X, Han K (2019) Apparent kinetic and thermodynamic calculation for thermal degradation of stearic acid and its esterification derivants through thermogravimetric analysis. Renew Energy 133:373–381
26. Conceicao MM, Fernandes VJ, Bazerra AF, Silva MCD, Santos IMG, Silva FC, Souza AG (2007) Dynamic kinetic calculation of castor oil biodiesel. J Therm Anal Calorim 87:865–869
27. Doyle CD (1962) Estimating isothermal life from thermogravimetric data. J Appl Polym Sci 6(24):639–642
28. Zheng S, Kates M, Dube MA, Mclean DD (2006) Acid-catalyzed production of biodiesel from waste frying oil. Biomass Bioenergy 30:267–272
29. Tan HY, Abdullah MO, Nolasco-Hipolito C (2015) The potential of waste cooking oil-based biodiesel using heterogeneous catalyst derived from various calcined eggshells coupled with an emulsification technique: a review on the emission reduction and engine performance. Renew Sust Energ Rev 47:589–603
30. Taufiq-Yap YH, Abdullah NF, Basri M (2011) Biodiesel production via transesterification of palm oil using NaOH/Al_2O_3 catalysts. Sains Malaysiana 40:587–594
31. Betiku E, Okeleye AA, Ishola NB, Osunleke AS, Ojumu TV (2019) Development of a novel mesoporous biocatalyst derived from kola nut pod husk for conversion of *Kariya* seed oil to methyl esters: a case of synthesis, modeling and optimization studies. Catal Lett:1–16
32. Siatis NG, Kimbaris AC, Pappas CS, Tarantilis PA, Polissiou MG (2006) Improvement of biodiesel production based on the application of ultrasound: Monitoring of the procedure by FTIR spectroscopy. J Am Oil Chem Soc 83(1):53–57
33. Rocha JG Jr, dos Santos MDR, Madeira FB, Rocha SFLS, Bauerfeld GF, da Silva WLG, Salomao AA, Tubino M (2019) Influence of fatty acid methyl ester composition, acid value, and water content on metallic copper corrosion caused biodiesel. J Braz Chem Soc 30(8):2–11
34. Serrano M, Oliveros R, Sanchez M, Moraschini A, Matinez M, Aracil J (2014) Influence of blending vegetable oil methyl esters on biodiesel fuel properties: oxidative stability and cold flow properties. Energy 65:109–115
35. Santos AGO, Araujo, Caldeira VPS, Fernandes VJ, Souza ID, Barros AK (2010) Model-fre kinetics applied to volatilization of Brazilian sunflower oil and its respective biodiesel. Thermochim Acta, 57-61.
36. Li H, Niu S, Lu C, Wang Y (2015) Comprehensive investigation of the thermal degradation characteristics of biodiesel and its feedstock through TGA-FTIR. Energy Fuel 29:5145–5153
37. Vyazovkin S (2000) Computational aspects of kinetic analysis. Part C. The ICTAC kinetics Project- the light at the end of the tunnel? Thermochim Acta 355:155–163
38. Naqvi SR, Hameed Z, Tariq R, Taqvi SA, Ali I, Niazi MBK (2019) Synergistic effects on co-pyrolysis of rice husk and sewage sludge by thermal behavior, kinetics, thermodynamic parameters and artificial neural network. Waste Manag 85:131–140
39. Rodrigues JS, do Valle CP, de Araujo P, de Souza MA, de Queiroz, Malveira J, Ricardo NMPS (2017). Study of kinetics and thermodynamic parameters of the degradation process of biodiesel produced from fish viscera oil. Fuel Process Technol, 161, 95-100.